# Clonotypic analysis of T cell reconstitution after haematopoietic stem cell transplantation (HSCT) in patients with severe combined immunodeficiency

H. Okamoto,* C. Arii,† F. Shibata,*
T. Toma,* T. Wada,* M. Inoue,*
Y. Tone,* Y. Kasahara,* S. Koizumi,*
Y. Kamachi,‡ Y. Ishida,§ J. Inagaki,⁋
M. Kato,** T. Morio†† and A. Yachie†

*Department of Pediatrics, Graduate School of
Medical Science, Kanazawa University,
†Department of Clinical Laboratory Science,
Division of Health Sciences, Graduate School of
Medical Science, Kanazawa University,
‡Department of Pediatrics, Nagoya University,
§Department of Pediatrics, Ehime University,
⁋Department of Pediatrics, Nara Medical
University, **Gunma Children's Medical Centre,
and ††Department of Pediatrics and
Developmental Biology, Tokyo Dental and
Medical University, Tokyo, Japan

## Summary

Haematopoietic stem cell transplantation (HSCT) is performed for treatment of a broad spectrum of illnesses. Reconstitution of an intact immune system is crucial after transplantation to avoid infectious complications, and above all, the establishment of T cell receptor (TCR) diversity is the most important goal in the procedure. Until recently, little has been known of the mechanism of T cell reconstitution in the very early period after HSCT. In this study, we analysed TCR repertoires sequentially in four patients with severe combined immunodeficiency (SCID) before and after HSCT. In all patients, the TCR repertoires were extremely abnormal before HSCT, whereas after transplantation there was progressive improvement in TCR diversity, based on analysis of the TCR Vβ repertoire and CDR3 size distributions. Somewhat unexpectedly, there was a significant but transient expansion of TCR diversity 1 month after transplantation in all cases. Clonotypic analysis of TCRs performed in one case showed that many T cell clones shared identical CDR3 sequences at 1 month and that the shared fraction decreased progressively. These results indicate that early expansion of TCR diversity may reflect transient expansion of pre-existing mature T cells from the donor blood, independent of de novo T cell maturation through the thymus.

**Keywords:** SCID, HSCT, T cell reconstitution, TCR diversity

## Introduction

Hematopoietic stem cell transplantation (HSCT) is the treatment of choice for various haematological malignancies. Eradication of malignant cells is achieved by intense chemotherapy performed prior to HSCT, but post-transplantation is crucial to reconstitute a functional haematological system to permit development of donor stem cells. In particular, reconstitution of a potent immune system with a diverse repertoire of T cells is of critical importance for defence against infections and tolerance induction after HSCT [1]. HSCT is now performed not only for malignant disorders but also for various autoimmune disorders [2,3] and primary immunodeficiency diseases [4–6]. In such cases, failure of effective immune reconstitution increases the risk of infections and unfavourable complications, and thereby adds to the risk of recurrence of the original disease. Therefore, monitoring the status of T cell reconstitution and use of this information in treatment is important for successful HSCT.

Two distinct pathways of T cell reconstitution, thymus-dependent and thymus-independent, are thought to operate after HSCT [7,8]. Although T cell reconstitution through the thymus-dependent pathway first appears as early as 2 months after HSCT, it gradually increases in size and diversity over 1–2 years [7,9–11]. Quantitative recognition of the naive T cell population is usually possible 5 or 6 months after the procedure; the slow recovery of T cell numbers reflects the passage of T cells through thymic selection for discrimination between self and non-self antigens [7,12,13]. As Borghans *et al.* reported recently, successful long-term reconstitution depends on the quantity of this thymic output [14]. On the other hand, very rapid T cell reconstitution is observed in some cases, suggesting that thymus-independent expansion of donor-derived mature T cells can also occur [15–17]. These T cells, although limited in diversity, may contribute significantly to immune reconstitution very early after HSCT, at a time when thymus-derived T cells are unavailable.

**Table 1.** Clinical profiles and treatment characteristics of the patients.

| Patient | 1 | 2 | 3 | 4 |
|---|---|---|---|---|
| Diagnosis | Omenn syndrome | Atypical Omenn syndrome | T-B-SCID (with MFT) | Omenn syndrome |
| Clinical manifestation | Eczema, diarrhoea failure to thrive Hepatosplenomegaly Lymph node swelling | Bronchitis Acute otitis media | Bronchitis *Carinii pneumonia* | Eczema Acute otitis media Hepatosplenomegaly |
| Mutation | *RAG2* | *RAG1* | *Artemis* | *RAG1* |
| Age at diagnosis | 0 m | 10 m | 6 m | 3 m |
| Age at HSCT | 4 m | 13 m | 8 m | 7 m |
| Graft | UCB $29 \times 10^7$/kg | UCB $3.5 \times 10^7$/kg | Father's BM $6.1 \times 10^8$/kg | UCB $5.29 \times 10^7$/kg |
| Conditioning | Flu + Bu + ATG | Flu + Cy + TBI | Flu + Bu | Flu + LPAM + ATG |
| GVHD prophylaxis | CyA | FK506 + sMTX | FK506 + sMTX | CyA + mPSL |
| GVHD (treatment) | None | Skin grade IV (mPSL + MMF) | Skin grade II Gut grade III (mPSL + MTX) | Skin grade II |
| Complication | None | MRSA sepsis | None | *Mycobacterium avium* Complex infection |

UCB: umbilical cord blood; MFT: maternal fetal transfusion; GVHD: graft-*versus*-host disease; HSCT: haematopoietic stem cell transplantation.

In this study, we analysed T cell receptor (TCR) diversity sequentially before and after HSCT in four patients with severe combined immunodeficiency disorders. Detailed analysis of TCR diversity and clonotypes showed that a brief period of transient but relatively diverse T cell expansion occurs soon after HSCT in SCID patients.

## Methods

### Patient characteristics

The clinical characteristics and conditioning regimens for HSCT in four SCID infants are shown in Table 1. Patients 1, 2 and 4 had Omenn syndrome and related disorders with *RAG1/RAG2* gene mutations. Patient 1 had heterozygous mutations in both alleles of the *RAG2* gene and exhibited typical clinical manifestations. Patient 2 was atypical, in that neither peripheral eosinophilia nor expansion of activated T cells was prominent; furthermore, typical skin lesions were also absent, but a prolonged lower respiratory tract infection led to the correct diagnosis. Patient 3 had mutations in the *Artemis* gene, and *Pneumocystitis carinii* infection was found in this patient. Patient 4 had homozygous mutations in *RAG1* that resulted in a frameshift and elimination of functional enzyme activity. However, multiple second-site mutations in oligoclonal T cells caused Omenn syndrome-like clinical manifestations [18]. Three patients received cord blood stem cell transplantation (CBSCT) and one patient received a haplo-identical bone marrow transplant (BMT) from his father. All these grafts were unmanipulated and were not devoid of mature T cells. All patients received non-myeloablative conditioning before transplantation; however, despite prophylaxis for

graft-*versus*-host disease (GVHD), three patients developed GVHD and one of these patients received methylprednisolone and mycophenolate mofetil (MMF). Approval for the study was obtained from the Human Research Committee of Kanazawa University Graduate School of Medical Science, and informed consent was obtained according to the Declaration of Helsinki.

### Flow cytometry

Surface antigens expressed on lymphocytes were analysed by flow cytometry. After red blood cell (RBC) lysis and washing in phosphate-buffered saline (PBS), peripheral blood samples were incubated with monoclonal antibodies for 15 min on ice. Phycoerythrin (PE)-conjugated anti-CD3 and anti-CD20 antibodies were obtained from BD Pharmingen (San Diego, CA, USA), and PE-conjugated anti-CD4 and anti-CD8 antibodies were products of Dako (Glostrup, Denmark). Fluorescein isothiocyanate (FITC)-conjugated anti-CD16 antibody was purchased from Immunotech (Marseille, France) and FITC-conjugated anti-CD45RO antibody was obtained from Dako. After washing twice in PBS, cells were analysed with a flow cytometer [fluorescence activated cell sorter (FACSCalibur); Becton Dickinson, San Diego, CA, USA]. The resulting data were analysed using CELLQUEST software (Becton Dickinson).

The T cell receptor (TCR) Vβ repertoire distribution was analysed using three-colour flow cytometry. After RBC lysis and washing in PBS, samples were incubated with appropriate PE-conjugated monoclonal antibodies with specificity for TCR Vβ (Immunotech) for 30 min on ice, followed by FITC-conjugated anti-CD8 antibody (Becton Dickinson) and R-phycoerythrin-Cy5-conjugated anti-CD4 antibody

(Dako) for 15 min. After washing in PBS, three-colour analysis was performed with the FACSCalibur instrument.

## Total RNA extraction and reverse transcription–polymerase chain reaction (RT–PCR)

Total RNA was extracted as described previously with a slight modification [19]. Briefly, peripheral blood mononuclear cells (PBMCs) were separated from heparinized peripheral blood by Ficoll-Hypaque density centrifugation. T cells were separated from PBMCs by the E-rosette method. CD4⁻ and CD8⁻ T cells were purified from T cells by negative selection using anti-CD8 or anti-CD4 magnetic beads (Dynal ASA, Oslo, Norway) [20]. The fraction of contaminating CD4⁺ T cells within the CD4-depleted cells or CD8⁺ T cells within the CD8-depleted cells was always less than 1% after the negative selection procedure. Total cellular RNA was isolated with Trizol reagent following the manufacturer's instructions (Gɪʙco BRL, Bethesda, MD, USA). The RNA was reverse-transcribed into cDNA in a reaction containing RandamHex Primer (TaKaRa, Otsu, Japan) and RAV-2 (TaKaRa). The concentration of RNA was measured using a GeneQuant pro RNA/DNA Calculator (Amersham Pharmacia Biotech, Cambridge, UK).

## CDR3 size analysis

CDR3 spectratyping was performed as described previously [20]. Briefly, cDNA was PCR-amplified through 35 cycles (94°C for 1 min, 55°C for 1 min and 72°C for 1 min) with a primer specific to 24 different Vβ subfamilies (Vβs 1–20 and Vβs 21–24) and a fluorescent Cβ primer. The fluorescent PCR products were mixed with formamide and a size standard (GeneScan-500 Tamra, Applied Biosystems, Foster City, CA, USA). After denaturation for 2 min at 90°C, the products were analysed with an automated 310 DNA sequencer and GeneScan software (Applied Biosystems). The overall complexity within a Vβ subfamily was determined by counting the number of discrete peaks and determining their relative size on the spectratype histogram, as described previously [21]. In this analysis, the complexity score = (sum of all peak heights/sum of major peak heights) × (number of major peaks); major peaks were defined as those peaks on the spectratype histogram with an amplitude of at least 10% of the sum of all peak heights. Numbers of undetectable Vβ subfamilies and mean complexity scores for detectable Vβ subfamily were calculated. The mean complexity scores ranged from 4·9 to 5·2 in healthy adult controls, as reported previously [22].

## TCR CDR3 cloning and sequence

PCR products of selected Vβ cDNA were electrophoresed on an agarose gel and purified using a QIAquick Gel Extraction Kit (Qiagen, Tokyo, Japan), followed by cloning with a Topo

TA Cloning Kit (Invitrogen, Carlsbad, CA, USA). Colonies containing the insert fragment were selected randomly. After purification with a QIAprep Spin Miniprep Kit (Qiagen) the recombinant plasmids were subjected to fluorescence dye terminator cycle sequencing, and the sequence reactions were analysed on a 3100 DNA sequencer (Applied Biosystems) after removal of unincorporated fluorescence dye using a Centri-Sep Spin Column (Applied Biosystems).

## Three-dimensional graphic display of TCR diversity through combination of CDR3 size analysis and Vβ repertoire distribution

Qualitative alterations of TCR Vβ repertoires obtained by CDR3 spectratyping were combined with the quantity of specific Vβ⁺ CD4⁺ and CD8⁺ T cells for each Vβ subfamily and plotted as landscape columns, as described previously [23].

## Results

### Lymphocyte subset

CD3⁺ T cells constituted the majority of lymphocyte populations prior to transplantation in patients 1 and 4, who both showed typical symptoms of Omenn syndrome (Table 2). In both cases, virtually all CD4⁺ T cells and CD8⁺ T cells expressed CD45RO⁺ memory phenotypes. In contrast, the numbers of CD3⁺ T cells were low compared to the numbers of lymphocytes in patients 2 and 3; in patient 3 the detectable T cells prior to transplantation were of maternal origin, as determined by microsatellite polymorphism analysis (data not shown). Most CD4⁺ T cells expressed CD45RO, whereas CD45RO expression on CD8⁺ T cells remained relatively low in these patients. Although CD4⁺ T cells increased progressively after HSCT in all cases, recovery of CD8⁺ T cells was delayed, especially in patient 2, who suffered severe GVHD. In each case, CD45RO⁺ T cells were predominant in the early stage after transplantation, whereas CD45RO⁻ T cells started to increase 9 months after transplantation.

### TCR Vβ repertoire distributions

Before transplantation, TCRVβ repertoires were restricted in both the CD4⁺ and CD8⁺ T cell populations in all patients (Fig. 1a,b, respectively). Oligoclonal T cell expansions were particularly prominent in patients 1 and 4, who showed typical symptoms of Omenn syndrome. After HSCT the TCRVβ repertoire distributions became diverse in all patients, and CD4⁺ T cells maintained the diversity of the TCRVβ repertoire until 9 months after transplantation. In contrast, CD8⁺ T cells showed evidence of oligoclonal expansion of limited clones: Vβ6⁺ and Vβ14⁺ cells in patient 2, Vβ6⁺ cells in patient 3 and Vβ8⁺ and Vβ12⁺ cells in patient 4 had all increased significantly at 4 months. However, the

**Table 2.** Changes in lymphocyte subpopulations.

| Patient | Subset | Pre | 1 m | 4 m | 9 m |
|---|---|---|---|---|---|
| 1 | WBC | 4 100 | 13 400 | 6 400 | 9 200 |
| | Lymph | 1 262 | 670 | 2 611 | 5 336 |
| | CD3 | 1 079 | 369 | n.d. | 3 431 |
| | CD4 | 721 | 320 | n.d. | 2 423 |
| | CD45RO$^+$/CD4 (%) | 97·7 | 84·9 | n.d. | 8·7 |
| | CD8 | 345 | 46 | n.d. | 662 |
| | CD45RO$^+$/CD8 (%) | 93·0 | 42·5 | n.d. | 2·6 |
| | CD16 | 92 | 301 | n.d. | 678 |
| | CD20 | 0 | 0 | n.d. | 1 233 |
| 2 | WBC | 2 800 | 9 800 | 16 000 | 6 900 |
| | Lymph | 1 300 | 1 800 | 2 000 | 1 800 |
| | CD3 | 334 | 1 015 | 1 786 | 1 336 |
| | CD4 | 289 | 749 | 1 732 | 1 219 |
| | CD45RO$^+$/CD4 (%) | 97·1 | 79·7 | 98·5 | 71·7 |
| | CD8 | 46 | 202 | 86 | 115 |
| | CD45RO$^+$/CD8 (%) | 44·4 | 51·8 | 64·1 | 56·2 |
| | CD16 | 965 | 718 | 110 | 328 |
| | CD20 | 1 | 2 | 104 | 137 |
| 3 | WBC | 3 200 | 7 400 | 4 600 | 10 600 |
| | Lymph | 512 | 1 110 | 1 242 | 2 600 |
| | CD3 | 73 | 931 | 1 098 | 2 428 |
| | CD4 | 67 | 380 | 452 | 991 |
| | CD45RO$^+$/CD4 (%) | 88·8 | 59·8 | 68·5 | 31·5 |
| | CD8 | 14 | 520 | 653 | 1 446 |
| | CD45RO$^+$/CD8 (%) | 5·9 | 34·9 | 38·5 | 19·6 |
| | CD16 | 440 | 178 | 139 | 122 |
| | CD20 | 0 | 1 | 1 | 10 |
| 4 | WBC | 26 600 | 8 100 | 7 500 | 10 000 |
| | Lymph | 19 600 | 400 | 1 020 | 6 300 |
| | CD3 | 18 855 | 111 | 755 | 3 780 |
| | CD4 | 9 114 | 84 | 609 | 2 905 |
| | CD45RO$^+$/CD4 (%) | 99·8 | 70·2 | 91·5 | 15·9 |
| | CD8 | 10 251 | 27 | 86 | 870 |
| | CD45RO$^+$/CD8 (%) | 99·8 | 72·5 | 71·8 | 2·8 |
| | CD16 | 725 | 289 | 95 | 485 |
| | CD20 | 20 | 0 | 171 | 2 035 |

WBC: white blood cells; n.d.: not done. All lymphocyte numbers represent absolute numbers/μl. CD45RO (%) shows percentages of CD45RO$^+$ cells within each lymphocyte subset.

diversity of the repertoire improved markedly at 9 months, except in patient 3, who showed a sustained increase in Vβ6$^+$ CD8$^+$ T cells.

## CDR3 size distribution

Representative profiles of CDR3 size distributions from patients 3 and 4 are shown in Fig. 2. One month after transplantation, the CDR3 size distributions showed an almost normal pattern for both the CD4$^+$ and CD8$^+$ T cell subsets. In particular, CD4$^+$ T cells from patient 3 showed completely normal patterns of CDR3 size distribution throughout the observation period. Although Vβ9$^+$ CD4$^+$ and Vβ13·2$^+$ CD4$^+$ T cells from patient 4 showed somewhat limited diversity at 1 and 4 months post-HSCT, the patterns had improved

significantly by 9 months. In marked contrast to CD4$^+$ T cells, CDR3 distributions within CD8$^+$ T cells were extremely skewed at 4 months in both patients, but the skewing of the CDR3 size distribution for CD8$^+$ T cells also improved significantly at 9 months. Patients 1 and 2 showed essentially similar patterns of changes in CDR3 size distributions.

## Complexity score (CS) for the TCRVβ CDR3 size distribution

The diversities of CDR3 size distributions were expressed as a complexity score (CS) and plotted for each TCR Vβ repertoire (Fig. 3). Sequential changes of CS for all patients are shown in Fig. 3. CS for CD4$^+$ T cells reached an almost normal level 1 month after HSCT and the values remained

(a)



(b)
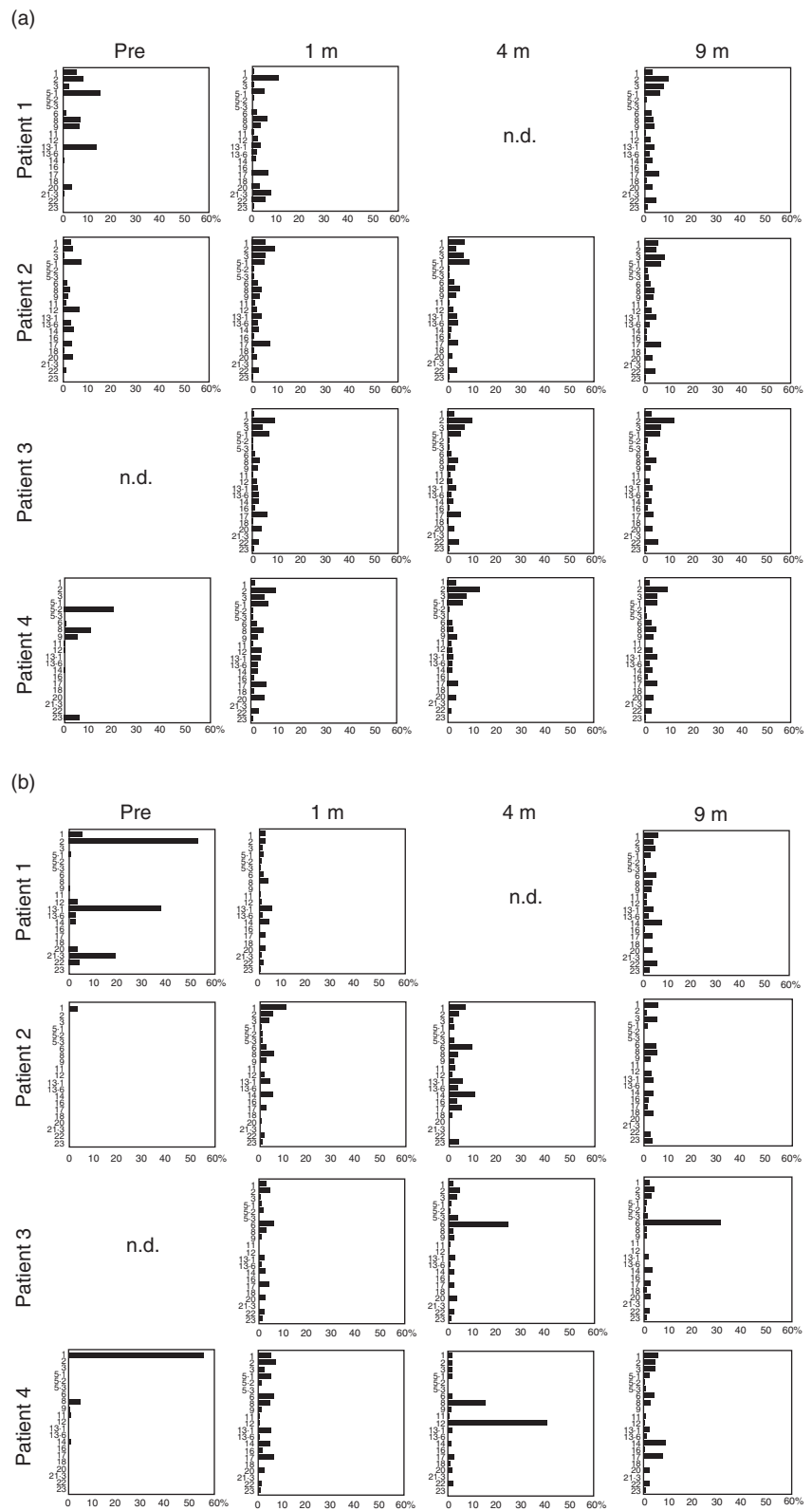


**Fig. 1.** Sequential changes in T cell receptor (TCR) Vβ repertoire distribution. TCR Vβ repertoire distributions for CD4+ T cells (a) and CD8+ T cells (b) were determined by a flow cytometry.

high in patients 1–3. In patient 4, in whom *Mycobacterium avium* complex infection persisted for several months, the CS improved after HSCT but remained low at 1 month. However, the CS increased progressively thereafter and reached a normal level at 9 months. Patient 2 experienced grade IV GVHD, and significant proportions of the Vβ repertoire showed a low CS or were undetectable at 4 and 9 months post-HSCT. The CS for CD8+ T cells improved
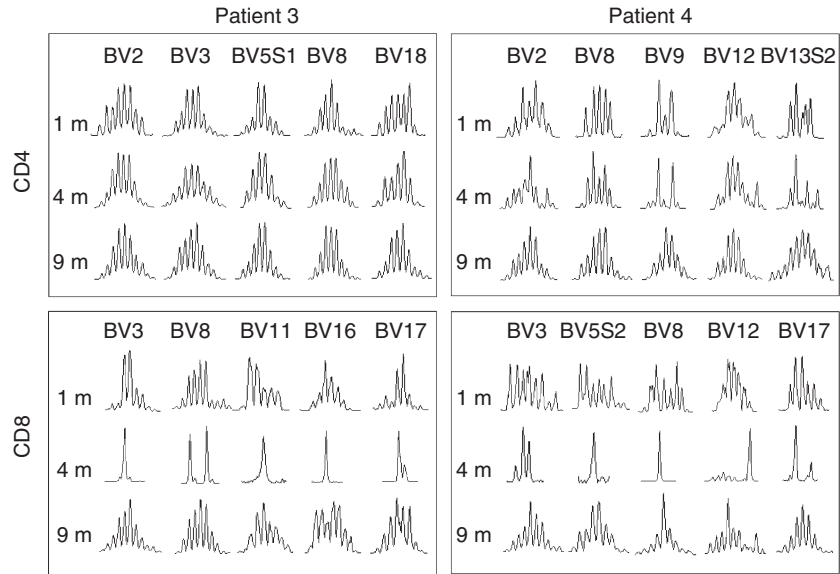
**Fig. 2.** Representative profiles of CDR3 size distribution after haematopoietic stem cell transplantation (HSCT). Representative profiles of the CDR3 size distributions from patients 3 and 4 are shown at 1, 4 and 9 months after HSCT. Five independent Vβ repertoires were chosen as representative profiles for CD4$^+$ T and CD8$^+$ T cells.

markedly at 1 month in all patients; however, in contrast to CD4$^+$ T cells, the CS for CD8$^+$ T cells decreased significantly after 4 months, but then increased again at 9 months. Recovery of the CS for CD8$^+$ T cells was delayed in patient 2.

## Combined qualitative and quantitative analysis of TCR repertoires

An improved visual representation was obtained by combining the results of TCR Vβ repertoire distributions and CDR3 size distributions, and this allowed analysis of sequential changes in TCR diversities. In marked contrast to pre-HSCT data, which showed extremely limited TCR diversity, as highlighted by the scarcity of columns and lack of Gaussian distributions for each Vβ repertoire, the TCR diversity of CD4$^+$ T cells improved significantly at 1 month post-HSCT in all patients and the diversities were maintained until 9 months

after transplantation (Fig. 4a). However, the patterns in patient 2 showed slightly skewed distributions at 4 and 9 months. A similar improvement in TCR diversity was observed in CD8$^+$ T cells after 1 month, but TCR diversity became markedly limited at 4 months, with a significant loss of detectable columns and a predominance of certain columns. These patterns improved at 9 months in all cases, but recovery was incomplete in patient 2 (Fig. 4b).

## DNA sequence analysis in the TCRVβ CDR3 region

DNA sequences in the CD4$^+$ TCRVβ2 CDR3 region were analysed in patients 3 and 4. This particular TCRVβ2 repertoire was chosen for analysis because of its high frequency within CD4$^+$ T cells, which enabled relatively easy acquisition of a large numbers of clones. In patient 3, eight of 56 clones obtained after 1 month were also detected in clones obtained
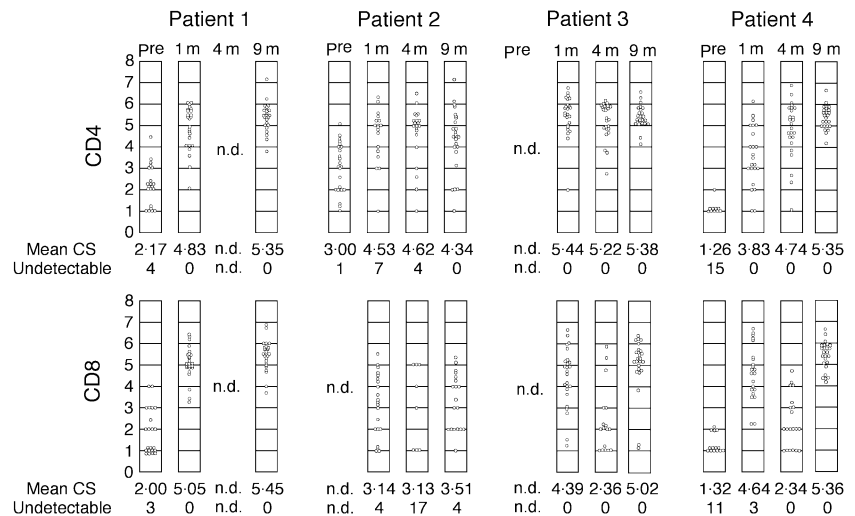


**Fig. 3.** Sequential changes in CDR3 complexity scores (CS). Complexity scores for each T cell receptor Vβ repertoire are shown. Each circle represents the CS for each repertoire; n.d.: not determined.
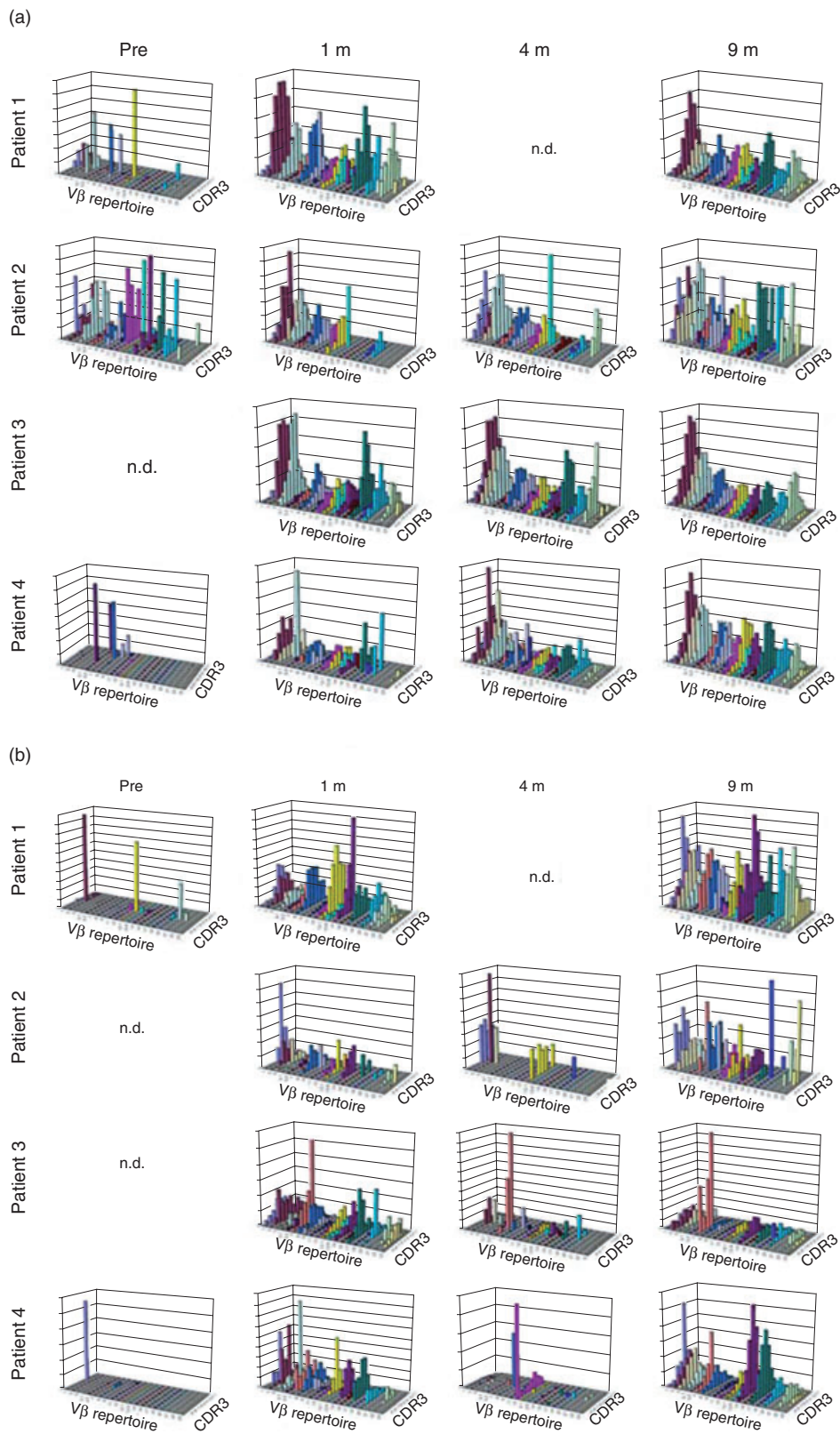
**Fig. 4.** Simultaneous combined display of T cell receptor (TCR) Vβ repertoire distribution and CDR3 size distribution. Data from qualitative analysis (CDR3 sizes) and quantitative analysis (TCR Vβ repertoires) are displayed visually as graphic landscape columns for CD4^{+} T cells (a) and CD8^{+} T cells (b). Identical Vβ repertoires are shown in the same colour. Values on the vertical axis are relative and do not represent absolute numbers; n.d.: not determined.

(a)

| Donor (Father's BM) | | | | 1 m | | | | 4 m | | | | 9 m | | | |
|---|---|---|---|---|---|---|---|---|---|---|---|---|---|---|---|
| BV | N-D-N | BJ | Frequency | BV | N-D-N | BJ | Frequency | BV | N-D-N | BJ | Frequency | BV | N-D-N | BJ | Frequency |
| CSA | RALTGLAGEDFYNEQF | FGPG | 1/137 | CSA | SPYSYLAVKMETQY | FGPG | 1/56 | CSA | PTHFIRPVSAYHQY | FGPG | 1/78 | CSA | RDGSGFLSSYNSPLH | FGNG | 1/53 |
| CSA | SGNRVGGSGANVLT | FGAG | 1/137 | CSA | RGQTPGRSTDTQY | FGPG | 2/56 | CSA | RSKLTNYGRAHEQF | FGPG | 1/78 | CSA | RVWDRAPSGANVLT | FGAG | 1/53 |
| CSA | VFPFLKTNTGELF | FGEG | 1/137 | CSA | SSYGTNRRDYEQF | FGPG | 1/56 | CSA | SGAGGAYSNQPQH | FGDG | 1/78 | CSA | REDGRSRYTGELF | FGEG | 1/53 |
| CSA | RDSLAGGSGELF | FGEG | 3/137 | CSA | AGADYYIEQIFW | FGPG | 1/56 | CSA | KTYKQSSSYEQY | FGPG | 1/78 | CSA | RVTSGRAVPDTQY | FGPG | 1/53 |
| CSA | RRGSSGAHNEQF | FGPG | 2/137 | CSA | RRGSSGAHNEQF | FGPG | 1/56 | CSA | SGTSGRVKYEQY | FGPG | 2/78 | CSA | RTPREGLNYGYT | FGSG | 2/53 |
| CSA | GDSRATYNEQF | FGPG | 1/137 | CSA | SPPLGGIDNEQF | FGPG | 1/56 | CSA | GDSRATYNEQF | FGPG | 1/78 | CSA | KRAGLNTGELF | FGEG | 1/53 |
| CSA | PRQGSNTGELF | FGEG | 2/137 | CSA | KVVGTVNNEQF | FGPG | 1/56 | CSA | FCRDGRYYGYT | FGPG | 1/78 | CSA | PRQGSNTGELF | FGEG | 1/53 |
| CSA | RDASRGTDTQY | FGPG | 3/137 | CSA | LDVAGGYNEQF | FGPG | 1/56 | CSA | RDPPGRYNEQF | FGPG | 1/78 | CSA | RPGLAGPYGQY | FGPG | 1/53 |
| CSA | YGLAGTYNEQF | FGPG | 1/137 | CSA | RDPGGYSYEQY | FGPG | 2/56 | CSA | YGLAGTYNEQF | FGPG | 1/78 | CSA | FQREWAYEQY | FGPG | 1/53 |
| CSA | ARQSLNTEAF | FGQG | 2/137 | CSA | ARQSLNTEAF | FGQG | 1/56 | CSA | ALAGVVDEQY | FGPG | 1/78 | CSA | RATGVMETQY | FGPG | 2/53 |
| CSA | PTSGRYNEQF | FGPG | 3/137 | CSA | KGTGKNNEQF | FGPG | 2/56 | CSA | PGAGANEKLF | FGSG | 1/78 | CSA | VTSGRLYEQY | FGPG | 1/53 |
| CSA | SAEDHTDTQY | FGPG | 3/137 | CSA | RVVGRGYEQY | FGPG | 3/56 | CSA | SGTGIFGGYT | FGSG | 1/78 | CSA | ERQLQETQY | FGPG | 1/53 |
| CSA | SSGTEETQY | FGPG | 3/137 | CSA | EGPNTGELF | FGEG | 2/56 | CSA | ATGMRNEPF | FGPG | 1/78 | CSA | SAGEYNEQF | FGPG | 2/53 |
| CSA | TDSNTGELF | FGEG | 5/137 | CSA | TDSNTGELF | FGEG | 3/56 | CSA | IPNGGDTQY | FGPG | 1/78 | CSA | TDSNTGELF | FGEG | 1/53 |
| CSA | TQTSTDTQY | FGPG | 3/137 | CSA | TSPGEDTQY | FGPG | 1/56 | CSA | PETDGYEQY | FGPG | 1/78 | CSA | AQNTGQQF | FGPG | 1/53 |
| CSA | ITRDYGYA | FGSG | 3/137 | CSV | PRVVVAEAF | FGQG | 2/56 | CSA | GLAADTQY | FGSG | 1/78 | CSA | RAPTGELF | FGEG | 1/53 |
| CSA | SYRVEKLF | FGSG | 2/137 | CSA | PPRRYEQY | FGPG | 1/56 | CSA | SYRVEKLF | FGSG | 1/78 | CSA | TPKGNIQY | FGAG | 1/53 |
| CSA | TGLFYEQY | FGPG | 2/137 | CSA | TGLFYEQY | FGPG | 2/56 | CSA | RDPTGELF | FGEG | 1/78 | CSA | DRESMQY | FGPG | 1/53 |
| CSA | TRRGYEQY | FGPG | 3/137 | CSA | TRRGYEQY | FGPG | 1/56 | CSA | EGGNTEAF | FGQG | 1/78 | CSA | RELDEQF | FGPG | 1/53 |
| CSA | IDLYTQY | FGPG | 1/137 | CSA | TSTAQRY | FGPG | 2/56 | CSA | RGQNTIY | FGEG | 1/78 | CSA | SLRGAF | FGQG | 1/53 |
| | Others | | 92/137 | | Others | | 25/56 | | Others | | 57/78 | | Others | | 30/53 |

(b)

| Donor (cord blood) | | | | 1 m | | | |
|---|---|---|---|---|---|---|---|
| BV | N-D-N | BJ | Frequency | BV | N-D-N | BJ | Frequency |
| CSA | YGQRDRVFDTGELF | FGEG | 2/124 | CSA | SGGHSTAGDSNTGELF | FGEG | 1/56 |
| CSA | KDRLAGKRFHEQY | FGPG | 2/124 | CSA | SPYSYLAVKMETQY | FGPG | 1/56 |
| CSA | RTGLAFNSDTQY | FGPG | 1/124 | CSA | RDGGRKSTGELF | FGEG | 3/56 |
| CSA | RVEEQATRDTQY | FGEG | 2/124 | CSA | KVTGGLSYGYT | FGSG | 1/56 |
| CSA | MGLAGSSYEQY | FGPG | 1/124 | CSA | LRAGGSNQPQH | FGDG | 1/56 |
| CSA | RDLRHRQETQY | FGPG | 1/124 | CSA | PPLAGPYNEQF | FGPG | 2/56 |
| CSA | RDQRTSAYTQY | FGEG | 1/124 | CSA | RDPSGGDNEQF | FGPG | 1/56 |
| CSA | RDRIGGTDTQY | FGPG | 1/124 | CSA | RDGTNNSPLH | FGKG | 1/56 |
| CSA | AGTSNVDTQY | FGPG | 6/124 | CSA | RGTSGYNEQF | FGPG | 2/56 |
| CSA | DTSRGAWEQY | FGQG | 2/124 | CSA | RLAGGSNEQF | FGQG | 2/56 |
| CSA | GSGGAQETQY | FGPG | 1/124 | CSA | RSGTSKNIQY | FGAG | 2/56 |
| CSA | GTSGSYNEQF | FGPG | 2/124 | CSA | RWGDSYNGQF | FGPG | 2/56 |
| CSA | YSGSRTDTQY | FGPG | 2/124 | CSA | PGQGLNEQF | FGPG | 1/56 |
| CSV | DGRPMNTEAF | FGQG | 2/124 | CSA | RGGRNQPQH | FGDG | 4/56 |
| CSA | DSRGFYEQY | FGPG | 1/124 | CSA | SSGTEERQY | FGPG | 5/56 |
| CSA | IMGNOFNQY | FGPG | 2/124 | CSA | SSGVTGELF | FGEG | 3/56 |
| CSA | PLAGGHEQF | FGPG | 2/124 | CSA | TDSNTGELF | FGEG | 1/56 |
| CSA | RAGEDYGYT | FGSG | 1/124 | CSA | RDTPNIQY | FGPG | 1/56 |
| CSA | TSGRYNEQF | FGPG | 1/124 | CSA | SGRGSTQY | FGPG | 1/56 |
| CSA | YNRENYGYT | FGSG | 2/124 | CSA | SGTGYEQF | FGPG | 1/56 |
| | Others | | 89/124 | | Others | | 20/56 |

**Fig. 5.** DNA sequence analysis in the CDR3 region. Polymerase chain reaction products of T cell receptor Vβ2 of CD4$^+$ T cells were subcloned and the CDR3 nucleotide sequences were determined. Amino acid sequences deduced from the nucleotide sequences are shown for data obtained from donor blood, and from blood collected 1 month, 4 months and 9 months post-haematopoietic stem cell transplantation (HSCT) for patient 3 (a). Similarly, data from donor blood and for 1 month post-HSCT are shown for patient 4 (b). Identical clones are highlighted with corresponding colours in (a).

from the donor, his father (Fig. 5a). Among 137 TCRVβ2 clones from the donor, 14 shared CDR3 sequences with clones obtained from the recipient at 1 month post-HSCT. Similarly, three of 78 and one of 53 clones obtained from the recipient at 4 and 9 months, respectively, were identical to clones derived from the donor. In contrast, none of the TCRVβ2 clones obtained from the CBSCT donor blood had identical sequences to clones obtained from patient 4 at 1 month post-HSCT (Fig. 5b).

## Discussion

Early reconstitution of the immune system is critical for the success of HSCT and for minimization of morbidity and mortality in SCID patients. Most transplantation-related complications, including herpes group virus infections, GVHD and thrombotic microangiopathy, occur very early after the procedure [24–26]. Recent findings indicate that at least some of these events are causally attributable to

immune dysfunction or delayed reconstitution of a normal immune system [27–29]. Impaired expansion of a diverse T cell repertoire may lead to severe infections, and a lack of regulatory T cells may be responsible for accelerated GVHD.

T cell reconstitution after HSCT occurs through two distinct mechanisms [7,8]: the thymus-dependent pathway of T cell reconstitution generally requires months after HSCT in SCID patients because the increase in naive T cells requires normalization of the size and function of the thymus [7,9–11]; in contrast, the thymus-independent pathway is dependent only on transient expansion of donor-derived mature T cells. Although T cell depletion has been used for HSCT to prevent GVHD in past procedures, an increasing number of reports indicate the benefits of T cell repletion, rather than depletion [8,30,31].

There are several pieces of evidence for early expansion of donor-derived mature T cells. First, the appearance of thymus-derived T cell clones in the peripheral blood is very unlikely within 1 month [7,9–11]; although immune reconstitution is reported to be fast following HSCT in infancy, it still takes 5–6 months for emergence of a sizeable number of CD45RO⁻ naive T cells with high T cell receptor excision circle (TREC) values. Secondly, most early T cells express a CD45RO⁺ memory phenotype, whereas *de novo* expansion of thymus-derived T cells clones presumably gives CD45RO⁻ cells [7–9]. Thirdly, microsatellite polymorphism analysis shows that early expanding T cells are mainly of donor origin and do not reflect expansion of residual recipient T cells [16,17]. These findings are highly suggestive of early, transient expansion of donor-derived T cells, regardless of their functional relevance. However, analysis of diversity in the early expanding T cell population has not been performed in detail, and there has been no direct evidence at a clonotypic level to show that clones within the circulation of the recipient are derived from mature T cells from the donor blood.

In this study, we chose patients with mutations in *RAG1/RAG2* or *Artemis* genes, because the SCID mutations, including *RAG1/RAG2*, *Artemis* and *IL2RG* gene mutations, result in similar thymus pathology and impaired output of functional T cells [32,33]. Our data show that early expansion of T cells with relatively high diversity does occur in the very early period after HSCT. These dynamic changes of TCR diversity were not accounted for fully by examination of the TCR Vβ repertoire distribution only, and the CDR3 size distribution analysis was superior for detection of the oligoclonality of the T cell population within a given Vβ repertoire. Furthermore, simultaneous display of these two parameters indicated clearly the transient nature of the TCR diversity, both quantitatively and qualitatively. The reason why TCR diversities for CD8⁺ T cells were reduced at 4 months is unclear; however, our data suggest that early expanding T cell populations are short-lived and disappear quickly from the circulation, to be slowly replaced subsequently by a thymus-derived *de novo* T cell population [7,16]. Although the thymus-derived T cells have high TCR

diversity, the absolute number of these T cells is still small at 4 months post-HSCT. Infections and alloantigen stimulation might have affected TCR diversities, as the skewing was more prominent in patients 2 and 4, who had severe GVHD and *M. avium* complex infection, respectively.

We showed further that the early expanding T cells are derived from mature T cells of donor origin. Although CDR3 nucleotide sequences were compared for only a limited number of clones, a markedly high fraction of clones shared identical sequences in patient 3. The progressive decline of the fraction of shared clones indicates that the early expanding peripheral T cells are replaced rapidly by thymus-derived *de novo* T cell clones. Because we analysed only a fraction of a vast number of clones belonging to each TCR Vβ family, it is statistically unlikely that identical clones would be found within the donor and recipient T cells without an extremely high overlap in clones between donor T cells and the patient's CD4⁺ T cells at 1 month post-HSCT. Presumably the adult CD4⁺ T cells have much less diversity than cord blood CD4⁺ T cells, and this permitted detection of overlapping clones in this study. In contrast, cord blood contains diverse clones of both CD4⁺ and CD8⁺ T cells; quantitatively, this is reflected in the large proportion of CD45RO⁻ naive T cells and high TREC values [13,34].

Considering that the present study was performed in only four cases with heterogeneous clinical characteristics, we should be cautious to draw any definitive conclusion. Nevertheless, the data shown here suggest the pivotal roles played by early expanding peripheral T cells. The functional significance of the early, transient expansion of donor-derived mature T cells is multifold. First, it may offer surrogate, but effective, protective immunity during the early post-HSCT period until potent immune function is reconstituted fully. Secondly, it may prevent adverse reactions to HSCT by providing regulatory functions to control excessive killer and inflammatory reactions evoked by allogeneic stimuli [35,36]; effective induction of immune tolerance may be dependent upon this function of peripheral T cells. Thirdly, our results may offer a rationale for manipulation of donor-derived mature T cells before infusion into the recipient, thereby promoting their beneficial effects, but reducing adverse functions [35,37,38]. Further detailed analyses of the nature of the early expanding T cells and techniques for *in vitro* manipulation of this potentially valuable population of donor T cells are mandatory for future improvement of HSCT.

## References

1 Auletta JJ, Lazarus HM. Immune restoration following hematopoietic stem cell transplantation: an evolving target. Bone Marrow Transplant 2005; **35**:835–57.

2 Isaacs JD, Thiel A. Stem cell transplantation for autoimmune disorders. Immune reconstitution. Best Pract Res Clin Hematol 2004; **17**:345–58.

3 Nash RA. Allogeneic HSCT for autoimmune diseases: conventional conditioning regimens. Bone Marrow Transplant 2003; **32** (Suppl. 1):S77–80.

4 Buckley RH, Schiff SE, Schiff RI et al. Hematopoietic stem-cell transplantation for the treatment of severe combined immunodeficiency. N Engl J Med 1999; **340**:508–16.

5 Slatter MA, Gennery AR. Umbilical cord stem cell transplantation for primary immunodeficiencies. Exp Opin Biol Ther 2006; **6**:555–65.

6 Grunebaum E, Mazzolari E, Porta F et al. Bone marrow transplantation for severe combined immunodeficiency. JAMA 2006; **295**:508–18.

7 Müller SM, Kohn T, Schulz AS, Debatin K-M, Friedrich W. Similar pattern of thymic-dependent T-cell reconstitution in infants with severe combined immunodeficiency after human leukocyte antigen (HLA)-identical and HLA-nonidentical stem cell transplantation. Blood 2000; **96**:4344–9.

8 Lewin SR, Heller G, Zhang L et al. Direct evidence for new T-cell generation by patients after either T-cell-depleted or unmodified allogeneic hematopoietic stem cell transplantations. Blood 2002; **100**:2235–42.

9 Patel DD, Gooding ME, Parrott RE, Curtis KM, Haynes BF, Buckley RH. Thymic function after hematopoietic stem-cell transplantation for the treatment of severe combined immunodeficiency. N Engl J Med 2000; **342**:1325–32.

10 Myers LA, Patel DD, Puck JM, Buckley RH. Hematopoietic stem cell transplantation for severe combined immunodeficiency in the neonatal period leads to superior thymic output and improved survival. Blood 2002; **99**:872–8.

11 Sarzotti N, Patel D, Li X et al. T cell repertoire development in humans with SCID after nonablative allogeneic marrow transplantation. J Immunol 2003; **170**:2711–8.

12 Roux E, Dumont-Girard F, Starobinski M et al. Recovery of immune activity after T-cell-depleted bone marrow transplantation depends on thymic activity. Blood 2000; **96**:2299–303.

13 Chen X, Barfield R, Benaim E et al. Prediction of T-cell reconstitution by assessment of T-cell receptor excision circle before allogeneic hematopoietic stem cell transplantation in pediatric patients. Blood 2005; **105**:886–93.

14 Borghans JA, Bredius RG, Hazenberg MD et al. Early determinants of long-term T-cell reconstitution after hematopoietic stem cell transplantation for severe combined immunodeficiency. Blood 2006; **108**:763–9.

15 van Leeuwen JEM, van Tol MJD, Joosten AM et al. Relationship between patterns of engraftment in peripheral blood and immune reconstitution after allogeneic bone marrow transplantation for (severe) combined immunodeficiency. Blood 1994; **84**:3936–47.

16 Roux E, Helg C, Dumont-Girard F, Chapuis B, Jeannet M, Roosnek E. Analysis of T-cell repopulation after allogeneic bone marrow transplantation: significant differences between recipients of T-cell depleted and unmanipulated grafts. Blood 1996; **87**:3984–92.

17 Wu CJ, Chillemi A, Alyea EP et al. Reconstitution of T-cell receptor repertoire diversity following T-cell depleted allogeneic bone marrow transplantation is related to hematopoietic chimerism. Blood 2000; **95**:352–9.

18 Wada T, Toma T, Okamoto H et al. Oligoclonal expansion of T lymphocytes with multiple second-site mutations leads to Omenn syndrome in a patient with RAG1-deficient severe combined immunodeficiency. Blood 2005; **106**:2099–101.

19 Mizuno K, Toma T, Tsukiji H et al. Selective expansion of CD16$^{high}$ CCR2$^-$ subpopulation of circulating monocytes with preferential production of haem oxygenase (HO)-1 in response to acute inflammation. Clin Exp Immunol 2005; **49**:1030–43.

20 Mizuno K, Yachie A, Nagaoki S et al. Oligoclonal expansion of circulating and tissue-infiltrating CD8$^+$ T cells with killer/effector phenotypes in juvenile dermatomyositis syndrome. Clin Exp Immunol 2004; **137**:187–94.

21 Konno A, Okada K, Mizuno K et al. CD8αα memory effector T cells descend directly from clonally expanded CD8α$^+$ β$^{high}$ TCRαβ T cells in vivo. Blood 2002; **100**:4090–7.

22 Wada T, Schuman SH, Garabedian EK, Yachie A, Candotti F. Analysis of T-cell repertoire diversity in Wiskott–Aldrich syndrome. Blood 2005; **106**:3895–7.

23 Yawalkar N, Ferenczi Jones DA et al. Profound loss of T-cell receptor repertoire complexity in cutaneous T-cell lymphoma. Blood 2003; **102**:4059–66.

24 Patel SR, Ridwan RU, Ortin M. Cytomegalovirus reactivation in pediatric hemopoietic progenitors transplant: a retrospective study on the risk factors and the efficacy of treatment. J Pediatr Hematol Oncol 2005; **27**:411–5.

25 Shimoni A, Yashurun M, Hardan I, Avigdor A, Ben-Bassat I, Nagler A. Thrombotic microangiopathy after allogeneic stem cell transplantation in the era of reduced-intensity conditioning: the incidence is not reduced. Biol Blood Marrow Transplant 2004; **10**:484–93.

26 Antin JH, Deeg HJ. Clinical spectrum of acute graft-vs.-host disease. In: Ferrara JLM, Cooke KR, Deeg HJ, eds. Graft-vs-host disease. New York: Marcel Dekker, 2005:369–81.

27 Liu C, He M, Rooney B, Kepler TB, Chao NJ. Longitudinal analysis of T-cell receptor variable β chain repertoire in patients with acute graft-versus-host disease after allogeneic stem cell transplantation. Biol Blood Marrow Transplant 2006; **12**:335–45.

28 Zorn E. CD4$^+$ CD25$^+$ regulatory T cells in human hematopoietic cell transplantation. Semin Cancer Biol 2006; **16**:150–9.

29 Barrett J. Improving outcome of allogeneic stem cell transplantation by immunomodulation of the early post-transplant environment. Curr Opin Immunol 2006; **18**:592–8.

30 Elmaagacli AH, Peceny R, Steckel N et al. Outcome of transplantation of highly purified peripheral blood CD34$^+$ cells with T-cell add-back compared with unmanipulated bone marrow or peripheral blood stem cells from HLA-identical sibling donors in patients with first chronic myeloid leukemia. Blood 2003; **101**:446–53.

31 Bhattacharya A, Slatter MA, Chapman CE et al. Single centre experience of umbilical cord stem cell transplantation for primary immunodeficiency. Bone Marrow Transplant 2005; **36**:295–9.

32 Cavadini P, Vermi W, Facchetti F et al. AIRE deficiency in thymus of 2 patients with Omenn syndrome. J Clin Invest 2005; **115**:728–32.

33 Mostoslavsky G, Fabian AJ, Rooney S, Alt FW, Mulligan RC. Complete correction of murine Artemis immunodeficiency by lentiviral vector-mediated gene transfer. Proc Natl Acad Sci USA 2006; **103**:16406–11.

34 McFarland RD, Douek DC, Koup RA, Picker LJ. Identification of a human recent thymic emigrant phenotype. Proc Natl Acad Sci USA 2000; **97**:4215–20.

35 Hess AD. Modulation of graft-versus-host disease: role of regulatory T lymphocytes. Biol Blood Marrow Transplant 2006; **12**:13–22.

36 Rezvani K, Mielke S, Ahmadzadeh M *et al.* High donor *FOXP3*-positive regulatory T-cell ($T_{reg}$) content is associated with a low risk of GVHD following HLA-matched allogeneic SCT. Blood 2006; **108**:1291–7.

37 Barber LD, Madrigal JA. Exploiting beneficial alloreactive T cells. Vox Sang 2006; **91**:20–7.

38 Karim M, Feng G, Wood KJ, Bushell AR. CD25$^+$ CD4$^+$ regulatory T cells generated by exposure to a model protein antigen prevent allograft rejection: antigen-specific reactivation *in vivo* is critical for bystander regulation. Blood 2005; **105**:4871–7.